Earth Observation–Based Geospatial Analysis of Population–Air Quality Interaction

Xuejia Wei[1],Zechang Li[2],Liang Huo[1],Tao Shen[1],Jiahui Wang[1],Jinlong Wang[1]

1.School of Geomatics and Urban Spatial Informatics, Beijing University of Civil Engineering and Architecture, No. 15, Yongyuan Road, Huangcun Town, Daxing District, Beijing, 102600, China;
2.Hebei Provincial Coalfield Geological Bureau New Energy Geological Team
weixuejia777@163.com;15235672164@163.com;huoliang@bucea.edu.cn;shentao@bucea.edu.cn;chenxin176615@gmail.com;wangjinlong202510@163.com

Keywords: Earth Observation;Geospatial Analysis;Air Quality Index(AQI);Population Density;Spatial Heterogeneity;Sustainable Urban Development

Abstract:

Against the backdrop of rapid urbanisation and environmental governance in megacities, understanding the spatial interactions between population distribution and the Air Quality Index (AQI) is crucial for achieving sustainable urban development. Taking Beijing as the study area, this research integrates high-resolution air quality monitoring data from June 2025 with geographic information from the Seventh National Population Census to construct a geospatial analysis framework based on an Earth Observation (EO) perspective. By comparing three typical spatial interpolation algorithms—Ordinary Kriging, Simple Kriging and Spline interpolation—this paper quantitatively characterises the spatial heterogeneity of Beijing's AQI and provides an in-depth analysis of the overlapping effects of population density and environmental exposure risk. The study found that: (1) when handling AQI data, which exhibits strong spatial autocorrelation, the Ordinary Kriging method yields the smallest root mean square error (RMSE) and demonstrates the best robustness; (2) the distribution of AQI in Beijing exhibits a distinct 'higher in the south, lower in the north' stepped pattern, with complex quadratic trends along the east-west axis; (3) The city's core area (the six urban districts) exhibits distinct characteristics of dual exposure to both high population density and high pollution levels. This study provides crucial data support and scientific evidence for the optimised allocation of environmental resources and the implementation of differentiated emission reduction strategies in megacities.

1. Introduction

Rapid urbanization has become a defining global phenomenon, particularly in megacities where large-scale population concentration, industrial restructuring, and spatial reorganization have reshaped the interrelationships between regional demographics, environmental quality, and resource utilization. As a preeminent megacity and the core of national functions, Beijing has experienced a continuous surge in its permanent population and transportation density. This rapid modernization has concentrated industrial and domestic pollution sources, making air quality a critical bottleneck that constrains sustainable development, impacts public health, and hinders the city's evolution into a model of ecological civilization. Consequently, clarifying the spatial relationship between air quality and population distribution is of paramount practical importance for optimizing urban governance and safeguarding public welfare.

Driven by innovations in spatial information technology, the integration of Earth Observation (EO) and advanced geospatial modeling has opened new pathways for the dynamic monitoring and scientific assessment of complex urban systems. By leveraging multi-source remote sensing, ground-based monitoring, and spatial analysis, the academic community has achieved significant milestones in urban atmospheric research. Current literature focuses heavily on time-series forecasting, utilizing cutting-edge frameworks such as complex network theory[1], CNN-Bi-LSTM hybrid deep learning[2], and the Informer model[3] to enhance the accuracy of short-term pollution warnings. Furthermore, research by Ahmed et al. [4] has demonstrated that incorporating auxiliary variables—such as hydrological and meteorological data—into deep learning models can effectively overcome the limitations of single-source data and optimize predictive reliability[5].

Despite these breakthroughs, a critical gap remains: current research is predominantly skewed toward temporal precision, while systematic analyses of spatial heterogeneity at the urban scale remain scarce. Within megacities, population distribution is highly uneven and functional zones exhibit stark differences[6]; thus, the spatial pattern of air quality directly dictates exposure risks. Studies that overlook this spatial differentiation fail to fully capture the coupling patterns between the urban environment and its inhabitants[7]. To address this, the present study focuses on Beijing, employing multi-criteria geostatistical analysis to simulate the spatial evolution of the Air Quality Index (AQI) and population distribution. By identifying these spatial evolution patterns and their underlying mechanisms[8], this research aims to bridge the current analytical gap and provide scientific evidence for data-driven pollution control and the development of liveable cities.

2. Materials and methods

2.1 Study Area and Data Pre-processing

This study covers the entire territory of Beijing, encompassing all 16 administrative districts, including Dongcheng, Xicheng, Chaoyang and Haidian. The geographical scope spans the central urban area, the near-suburban plains and the distant suburban mountainous regions. Given the significant differences in topography and urban functional zoning, the area exhibits typical characteristics of spatial heterogeneity, making it suitable for conducting research on the spatial distribution of population and air quality. The study utilises two primary data sources: air quality monitoring data and population and geographical

data. These sources are authoritative and timely, meeting the requirements of the research, thereby laying a solid data foundation for subsequent spatial interpolation and statistical analysis.

Air Quality Index (AQI) data were obtained from 35 official air quality monitoring stations operated by the Beijing Municipal Ecological Environment Monitoring Centre. The spatial distribution of these monitoring stations is shown in Figure 1; the stations cover all functional zones across the city, encompassing the central urban area, suburban areas and ecological buffer zones, and the data are highly spatially representative. Given that meteorological fluctuations can interfere with the accurate identification of spatial patterns in air quality, this study excludes periods of extreme weather conditions and selects 11–17 June 2025 as the study period. The mean daily AQI concentrations at each monitoring station during this period are calculated and used as the subject of analysis; During this period, Beijing experienced predominantly stable weather conditions, with minimal fluctuations in meteorological factors such as wind speed and precipitation. This minimises external meteorological interference and accurately reflects the spatial distribution patterns of endogenous pollution caused by local emission sources.

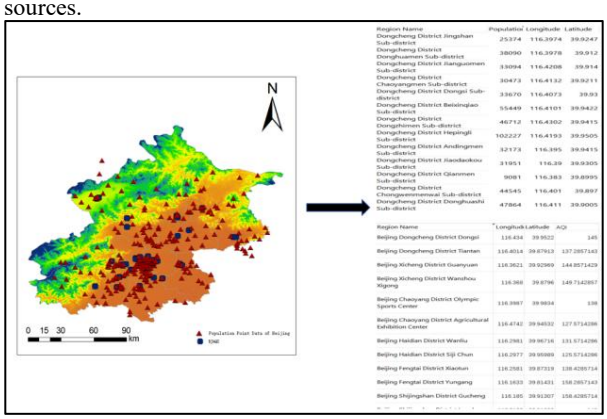

Fig. 1 Distribution of air quality and population data across 16 districts in Beijing

Population and geographical data were derived from the statistical data of the Seventh National Population Census, which was spatially matched against the administrative boundaries of Beijing. Relevant statistical data indicate that the rate of change in Beijing's permanent resident population between 2020 and 2025 was merely 0.22%. The spatial patterns of population concentration and dispersion have not undergone fundamental changes, and the continuity of spatial distribution is extremely strong. Therefore, utilising this census data for spatial analysis effectively ensures the reliability and accuracy of the research results, whilst avoiding biases in interpolation results caused by temporal fluctuations in population.

Data pre-processing is a critical step in ensuring the accuracy of spatial interpolation. Particularly for spatial statistical methods such as Kriging, the assumption that the observed data approximately follow a normal distribution is a core theoretical prerequisite. If the raw data exhibit skewed distributions or outliers, this will directly lead to distorted fitting of the variogram, weaken the capture of spatial autocorrelation characteristics, and significantly reduce the accuracy and stability of the interpolation predictions. Consequently, this study utilised the ArcGIS Geostatistical Analyst toolbar to conduct normality tests and data transformation on population point data and AQI monitoring data individually. Methods such as the Box-Cox transformation and logarithmic transformation were employed to correct data skewness, remove extreme outliers and impute missing data, thereby ensuring the data met the normal distribution assumption required for Kriging interpolation. Figure 2 illustrates the complete workflow for the normalisation of Beijing's population point data, comprising steps such as exploratory analysis of the raw data, normality testing, selection of the optimal transformation method, and validation of the transformed data. Following pre-processing, the structure of the variogram becomes more stable, effectively enhancing the goodness of fit and predictive accuracy of the subsequent interpolation model.

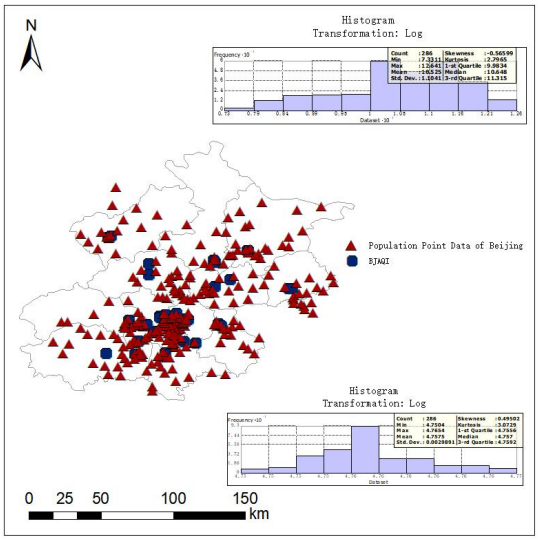

Fig. 2 Correlation between Beijing's population data and AQI data

2.2 Data Processing Methods

This study adopts a three-stage technical framework to investigate the spatial correlation between population distribution and air quality in Beijing, as shown in Figure 3. First, in the data collection phase, two core datasets are integrated: Beijing district-level 7th population census data and Beijing air quality monitoring station AQI (Air Quality Index) data, providing multi-source heterogeneous data support for subsequent spatial analysis. Second, in the spatial interpolation and error evaluation phase, three spatial interpolation methods—Ordinary Kriging Interpolation, Simple Kriging Interpolation, and Sample Interpolation—are applied to transform discrete AQI monitoring data into continuous spatial surfaces, followed by quantitative error evaluation and method comparison to identify the optimal interpolation scheme. Finally, in the correlation evaluation phase, the interpolated AQI spatial data is matched with population census data at the district level, and both Pearson Correlation Coefficient and Spearman Correlation Coefficient are employed to quantitatively assess the linear and monotonic rank-order correlations between population distribution and air quality, revealing their spatial association characteristics

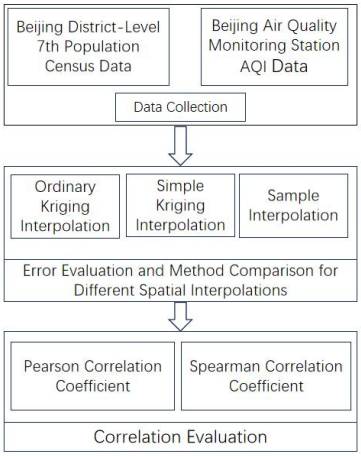

Fig. 3 Technology Roadmap

2.2.1 Ordinary Kriging Interpolation: The ordinary Kriging method assumes that the expected value of a spatial attribute is unknown; its core principle is to effectively capture the spatial autocorrelation characteristics of the variable through a semivariogram. The interpolation estimation formula can be expressed as:

$$Z^*(x_0) = \sum_{i=1}^{n} \lambda_i Z(x_i) \quad (1)$$

In the equation,$Z^*(x_0)$ represents the predicted value at the point of interest, and λ_i denotes the weighting coefficient corresponding to each sampling point. To ensure that the interpolation results satisfy the requirement of unbiasedness, the weight coefficients must satisfy the constraint $\sum\lambda_i = 1$. This method fully accounts for the spatial structural characteristics of the variables and can effectively handle monitoring station data with spatial bias, demonstrating high applicability and reliability in spatial distribution modelling.

2.2.2 Simple Kriging Interpolation: The simple Kriging method assumes that the global mean of the spatial attribute within the study area is a known constant (m). Compared to ordinary Kriging, this method captures the local variability of data with pronounced hierarchical or trend characteristics more accurately by first removing the global mean and then modelling the residuals using a semi-variogram. The interpolation estimate is expressed as follows:

$$Z^*(x_0) = \sum_{i=1}^{n} \lambda_i Z(x_i) + \left[1 - \sum_{i=1}^{n} \lambda_i\right] m \quad (2)$$

In the formula,$Z^*(x_0)$ represents the predicted value at the point of interest, $Z(x_i)$ represents the observed values at neighbouring sampling points, and λ_i denotes the corresponding weighting coefficient. By incorporating the known mean m, this formula effectively separates the global trend of the data from local spatial autocorrelation. It is particularly suitable for research subjects with pronounced spatial gradients, such as population distribution, and significantly enhances the ability of the interpolation results to capture local details.

2.2.3 Spline interpolation: Spline interpolation falls within the category of radial basis function interpolation. This method approximates measured sampling points by simulating the bending deformation of a flexible surface, and constructs a continuous, smooth spatial distribution surface based on function fitting. Compared to the Kriging series of interpolation methods, the core advantage of spline interpolation lies in the exceptional continuity and smoothness of the generated spatial surfaces. It can intuitively and clearly illustrate the spatial dispersion trends of variables such as pollutants, making it suitable for visualising spatial gradients; However, this method also has limitations. In areas where measured sampling points are sparse, numerical overshoot is highly likely to occur, causing predicted results to deviate from actual background values, and the accuracy of the interpolation may fluctuate to some extent.

3. Results

3.1 Ordinary Kriging

3.1.1 Analysis of Ordinary Kriging Interpolation Results: To reveal the spatial distribution patterns of Beijing's population, a quadratic trend surface analysis method was first employed to perform a global trend fit on the population point data (Figure 4). The results show that the population exhibits non-linear variation in both the X and Y directions: in the X direction, population values follow an arc-shaped distribution that rises initially and then declines; in the Y direction, the population shows a gradual increase as it extends north and south. with a distinct population peak forming in the central region. This clearly reflects the macro-level pattern of 'concentration in the centre and gradual decline towards the periphery'. This trend characteristic provides the foundation for subsequent trend removal and variational function modelling in the Kriging interpolation process.

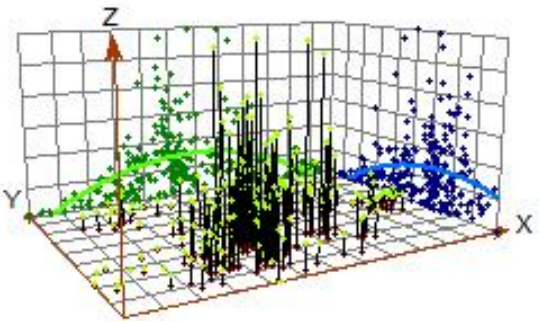

Fig. 4 Analysis of the secondary trends in the spatial distribution of Beijing's population

To verify the reliability and predictive accuracy of the ordinary Kriging interpolation model, a cross-validation analysis was conducted (Figure 5). This validation involved a total of 286 sample points. The statistical results show that the mean prediction error was 1913.724, the root mean square error (RMSE) was 44887.43, the mean standardised error was 0.0916, the root mean square standardised error was 0.8645, and the mean standard error was 49245.6. Judging from the scatter plot of measured and predicted values, the two exhibit a significant positive correlation (with a regression coefficient of approximately 0.404), indicating that the model is capable of capturing the overall trend of population spatial distribution; however, the scatter plot shows a certain degree of dispersion, reflecting local prediction biases, which are related to the spatial heterogeneity of the population data and the model parameter settings. Overall, the cross-validation results indicate that this interpolation model possesses a certain degree of reliability and can be used to characterise the spatial distribution of

Beijing's population; it also provides a basis for subsequent model optimisation.

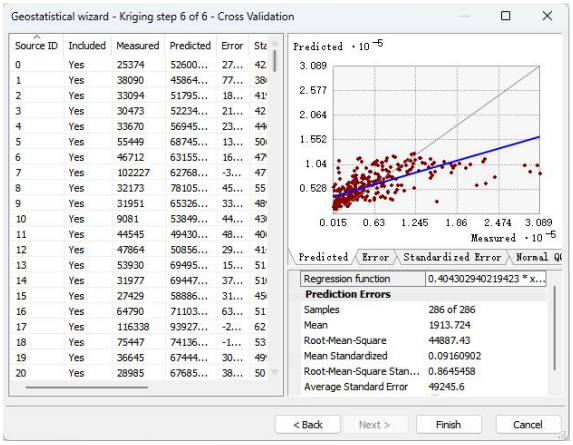

Fig. 5 Cross-validation results for ordinary Kriging interpolation

The raster map of Beijing's population distribution (Figure 6), derived using ordinary Kriging interpolation, clearly illustrates the city's monocentric, concentric distribution pattern, characterised by 'concentration in the core and a gradual decline towards the periphery'. Centred on the central urban area, a contiguous zone of high population density has formed, predominantly coloured red and deep orange, with values ranging from 95,873.66 to 257,396.29; this constitutes the population nucleus of the city; Moving towards the peripheral areas, population density decreases gradually with distance, with colours transitioning to light yellow and yellow-green, and values falling within the range of 13,282.01 to 55,377.48; The outlying suburbs are predominantly blue and cyan, with values mostly ranging from 967.89 to 13,282.01. These areas have the lowest population density, which aligns closely with topographical constraints and ecological functions, clearly illustrating the population siphoning effect of the capital's core functional area and the disparities in regional development.

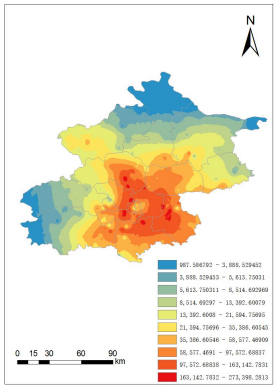

Fig. 6 Spatial distribution of Beijing's population based on ordinary Kriging interpolation

3.1.2 Analysis of AQI Results Using Ordinary Kriging Interpolation: To reveal the spatial distribution patterns of the Air Quality Index (AQI) in Beijing, a quadratic trend surface analysis method was first employed to perform a global trend fit on the AQI point data (Figure 7). The three-dimensional trend map reveals that the AQI exhibits non-linear variation in both the X and Y directions: along the X-axis, AQI values follow a gradually rising arc-shaped distribution, whilst along the Y-axis, they show a pattern of initially stable values followed by a gradual decline as they extend from north to south. A distinct high-AQI zone has formed in the southern region, clearly reflecting the macro-level pollution pattern of 'higher levels in the south and lower levels in the north'. This trend characteristic provides the foundation for subsequent trend removal and variational function modelling in the Kriging interpolation process.

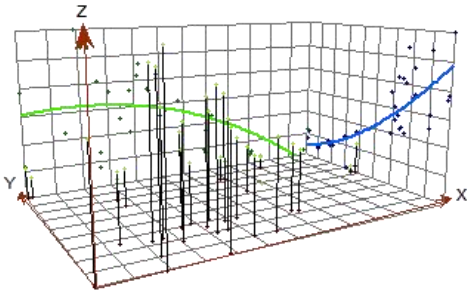

Fig. 7 Analysis of the quadratic trend in the spatial distribution of the AQI in Beijing

Building on this, a spatial distribution grid of Beijing's AQI was generated using ordinary Kriging interpolation (Figure 8) to further characterise the microspatial variations in air quality. The interpolation results clearly reveal a distribution pattern characterised by 'concentration in the south and a gradual decrease in the north': centred on the southern urban areas, a contiguous region of high AQI values has formed, predominantly coloured red and deep orange, with values concentrated in the higher ranges, constituting the city's core air pollution zone; Moving northwards, AQI values gradually decrease with distance, with colours transitioning to light yellow and yellow-green, and the numerical range dropping significantly; the northern outlying areas are predominantly blue and cyan, with values in the lowest range, consistent with the ecological barrier function and topographical dispersion conditions. Overall, this accurately depicts the spatial heterogeneity of Beijing's air quality.

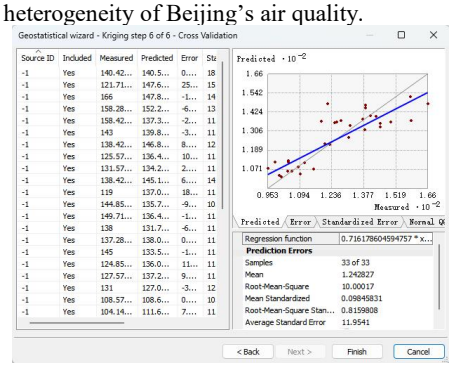

Fig. 8 Cross-validation of AQI using ordinary Kriging interpolation

To verify the reliability and predictive accuracy of the ordinary Kriging interpolation model, a cross-validation analysis was conducted (Figure 9). This validation involved a total of 33 sample points. The statistical results show that the mean prediction error was 1.242827, the root mean square error (RMSE) was 10.00017, the mean standardised error was 0.09845831, the root mean square standardised error was 0.8159808, and the mean standardised error was 11.9541. Judging from the scatter plot of measured and predicted values, the two exhibit a significant positive correlation (with a regression coefficient of approximately 0.756), indicating that the model is capable of capturing the overall trend of the spatial distribution of AQI; the scatter plot is relatively

concentrated, reflecting the model ' s strong ability to characterise the spatial heterogeneity of AQI. Overall, the cross-validation results indicate that this interpolation model possesses good reliability and can be used to characterise the spatial distribution features of AQI in Beijing, whilst also providing data support for subsequent air quality management and pollution source tracing analyses.

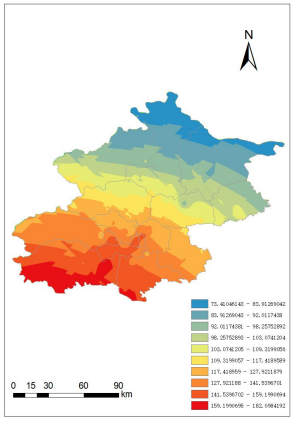

Fig. 9 Spatial distribution of the AQI in Beijing based on ordinary Kriging interpolation

3.2 Simple Kriging

3.2.1 Analysis of Simple Kriging Interpolation Results for Population Data: Prior to performing simple Kriging interpolation, it is necessary to model the spatial autocorrelation structure of the population data in order to determine the parameters of the variational function (Figure 10). In this modelling, the Stable model was adopted, with the block value set at 0.6212937, the partial base value at 0.3340073, the main range at 0.4999735, with no consideration given to anisotropy. Judging by the fit between the covariance curve and the discrete data points, the model successfully captures the spatial autocorrelation characteristics of the population data, providing a reliable spatial structural foundation for the subsequent simple Kriging interpolation

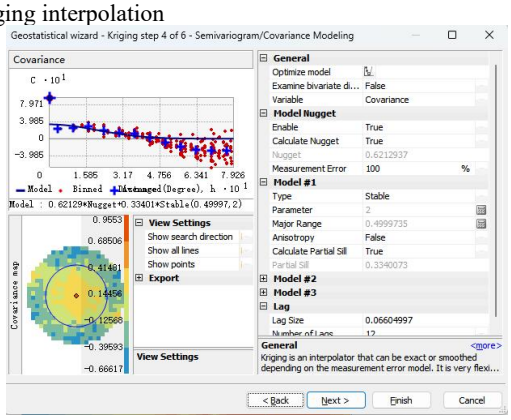

Fig. 10 Modelling using simple Kriging interpolation variational functions

Based on the above variational function model, simple Kriging was employed to perform spatial interpolation of Beijing's population, yielding a population distribution raster (Figure 11). The interpolation results clearly illustrate a monocentric, concentric distribution pattern characterised by 'concentration in the core and a gradual decline in the periphery': with the central urban area at its core, a contiguous zone of high population density has formed, predominantly coloured in red and deep orange, with values concentrated in the higher range; moving towards the peripheral areas, population density gradually decreases with distance, with colours transitioning to light yellow and yellow-green; the far-suburban areas are predominantly blue and cyan, with the lowest population density, which aligns closely with topographical constraints and ecological functional positioning, intuitively reflecting the population siphoning effect of the capital's core functional area and regional development disparities.

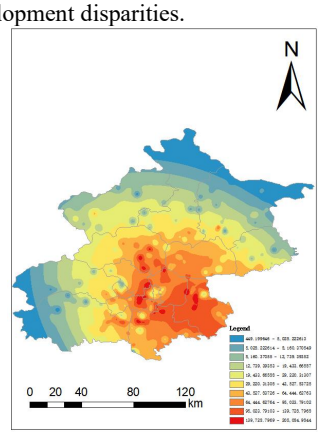

Fig. 11 Spatial distribution of Beijing's population based on simple Kriging interpolation

3.2.2 Analysis of AQI Results Using Simple Kriging Interpolation: Prior to performing simple Kriging interpolation on Beijing's AQI data, a spatial autocorrelation model must first be constructed to characterise its spatial structure (Figure 12). In this modelling, a Stable model was adopted, with a block weight of 0.003631976 and a partial base weight of 0.001277601, with a principal range of 0.1202114; anisotropy was not taken into account. Judging by the fit between the covariance curve and the discrete data points, the model successfully captures the spatial autocorrelation characteristics of the AQI data, providing a reliable spatial structural foundation for subsequent interpolation.

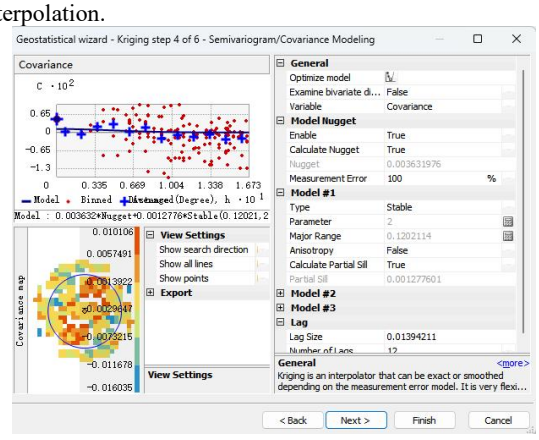

Fig. 12 Modelling of the variational function using simple Kriging interpolation for Beijing's AQI

Based on the above variational function model, spatial interpolation of Beijing's AQI was performed using the simple Kriging method, yielding a grid of air quality distributions (Figure 13). The interpolation results clearly reveal a gradient distribution pattern characterised by 'higher values in the south and lower values in the north': centred on the southern region, a contiguous area of high AQI values has formed, predominantly coloured red and deep orange, with

values concentrated in the range of 162.29–183.65; moving northwards, AQI values gradually decrease with distance, and the colours gradually change to light yellow and yellow-green; the northern outlying areas are predominantly blue and cyan, with values in the lowest range of 71.49–82.55. This pattern aligns closely with the topographical dispersion conditions and the ecological function of these areas, providing a clear illustration of the spatial heterogeneity of Beijing's air quality

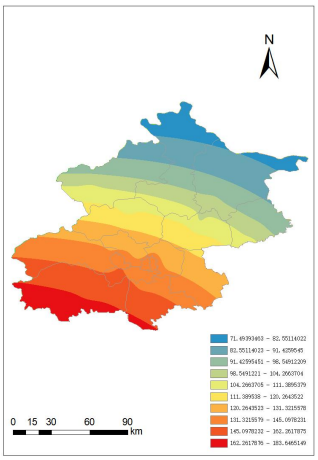

Fig. 13 Spatial distribution of the AQI in Beijing based on simple Kriging interpolation

3.3 Spline interpolation

3.3.1 Analysis of the results of the Spline interpolation of population data: The spatial distribution of population residuals obtained via spline interpolation (Figure 14) provides a visual representation of the deviation characteristics between the model's predicted values and the observed values. The overall residuals are predominantly found in light yellow areas with values close to zero, indicating that the model fits the global population trend with a high degree of accuracy; However, there are distinct clusters of residuals in localised areas: small pockets of high positive residuals (pink and light brown) appear in the core area of the south-east, whilst low negative residuals (green) are distributed across the north-east and south. This spatial heterogeneity not only reflects the localised clustering characteristics of population distribution but also highlights the limitations of spline interpolation in capturing the details of extremely dense areas.

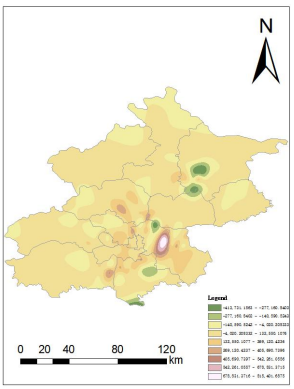

Fig. 14 Spatial distribution of residuals from spline interpolation of Beijing's population

3.3.2 Analysis of AQI Results Using Spline Interpolation: The spatial distribution of AQI residuals obtained via spline interpolation (Figure 15) clearly illustrates the spatial pattern of air quality prediction errors. Overall, the residuals are predominantly light yellow, indicating near-zero values, which suggests that the model fits the macro-scale gradient changes in AQI well; A distinct area of low negative residuals (green) has formed in the western mountainous regions, whilst contiguous areas of high positive residuals (pink and light brown) have emerged in the eastern plains. This distribution is closely related to topographical dispersion conditions and the spatial distribution of pollution sources, reflecting the bias characteristics of spline interpolation when characterising local heterogeneity in air quality.

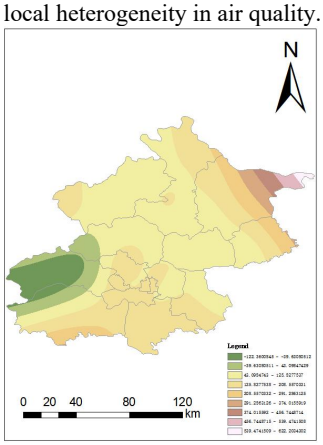

Fig. 15 Spatial distribution of AQI spline interpolation residuals in BeijingCaCl₂

4. Discussion

4.1 Single-Core Concentric Pattern of Population Distribution

The study reveals that Beijing ' s population distribution follows a distinct spatial gradient, forming a "single-core concentric" structure centered on the urban core. Population density is highest within the central functional zones and decreases progressively toward the periphery. This pattern highlights a significant agglomeration effect, where the capital ' s core areas exert a dominant pull on regional demographics and resources.

4.2 South-to-North Spatial Differentiation of AQI

The Air Quality Index (AQI) in Beijing exhibits a stark "higher in the south, lower in the north" differentiation. Pollution levels are consistently elevated in southern regions due to industrial concentration and transport density, whereas the northern ecological buffer zones maintain superior air quality. This spatial heterogeneity is closely aligned with the city's topographical dispersion conditions and its specialized functional zoning.

4.3 Applicability Assessment of Geostatistical Methods

Both Ordinary and Simple Kriging methods effectively capture the spatial autocorrelation of population and AQI data. While spline interpolation excels in preserving the smooth continuity of spatial variations, cross-validation indicates that Kriging models provide higher reliability for variables with complex spatial structures. However, spline methods show noticeable prediction biases in high-density urban centers and rugged mountainous terrains.

5. Conclusion

The integration of trend analysis and variational modeling systematically characterizes the coupling between urban environments and population distribution. Residual analysis indicates that while the models accurately fit overall spatial trends, localized deviations persist in areas of high heterogeneity—specifically within the high-density urban core for population data and near industrial sources or mountainous terrain for AQI. These discrepancies stem from the inherent spatial non-stationarity of the urban fabric and the complexity of micro-scale environmental factors.

To address these limitations, future research should focus on optimizing the parameters of variational functions and incorporating auxiliary variables such as land-use types, transportation network density, and building morphology. Utilizing advanced techniques like Co-Kriging or hybrid deep learning models could further minimize local residuals and enhance the simulation of micro-scale spatial features.

Ultimately, these findings provide a scientific baseline for "refined urban governance" in Beijing. The observed AQI disparities suggest a need for targeted emission reductions and the development of ventilation corridors in the southern districts. Simultaneously, optimizing the spatial alignment between high-density populations and ecological resources will be critical for mitigating exposure risks and building a more liveable, ecologically resilient megacity.

References

[1] Ahmed, A.A., Jui, S.J., Sharma, E., Ahmed, M.H., Raj, N., Bose, A., 2023. An advanced deep learning predictive model for air quality index forecasting with remote satellite-derived hydro-climatological variables[J]. Science of The Total Environment, 885: 167234. https://doi.org/10.1016/j.scitotenv.2023.167234

[2] Bhandari, B., Mayer, T., 2025. Comparing deep learning models for mapping rice cultivation area in Bhutan using high-resolution satellite imagery[J]. ISPRS Open Journal of Photogrammetry and Remote Sensing, 15: 100084. https://doi.org/10.1016/j.ophoto.2025.100084

[3] Garcia, E., Johnston, J., McConnell, R., Palinkas, L., Eckel, S.P., 2023. California's early transition to electric vehicles: Observed health and air quality co-benefits[J]. Science of The Total Environment, 867: 161761. https://doi.org/10.1016/j.scitotenv.2023.161761

[4] Liu, J., Zheng, Y., Lee, C., 2024. Statistical analysis of the regional air quality index of Yangtze River Delta based on complex network theory[J]. Applied Energy, 357: 122458. https://doi.org/10.1016/j.apenergy.2024.122458

[5] Ma, S., He, J., He, J., Feng, Q., Bi, Y., 2024. Forecasting air quality Index in yan'an using temporal encoded Informer[J]. Expert Systems with Applications, 255: 124868. https://doi.org/10.1016/j.eswa.2024.124868

[6] Pedley, D., Morgenroth, J., 2025. Detecting and measuring fine-scale urban tree canopy loss with deep learning and remote sensing[J]. ISPRS Open Journal of Photogrammetry and Remote Sensing, 15: 100082. https://doi.org/10.1016/j.ophoto.2025.100082

[7] Rabie, R., Asghari, M., Nosrati, H., Niri, M.E., Karimi, S., 2024. Spatially resolved air quality index prediction in megacities with a CNN-Bi-LSTM hybrid framework[J]. Sustainable Cities and Society, 109: 105688. https://doi.org/10.1016/j.scs.2024.105688

[8] Sarkar, N., Gupta, R., Keserwani, P.K., Govil, M.C., 2022. Air Quality Index prediction using an effective hybrid deep learning model[J]. Environmental Pollution, 307: 120404. https://doi.org/10.1016/j.envpol.2022.120404